Resonant hyper-Raman and second-harmonic scattering in a CdS quantum-dot system

A. V. Baranov
Research Institute for Electronic Science, Hokkaido University, Sapporo 060, Japan
and S. I. Vavilov State Optical Institute, 199034, St. Petersburg, Russia

K. Inoue, K. Toba, and A. Yamanaka
Research Institute for Electronic Science, Hokkaido University, Sapporo 060, Japan

V. I. Petrov and A. V. Fedorov
S. I. Vavilov State Optical Institute, 199034, St. Petersburg, Russia
(Received 6 September 1995)

Excitation profiles of resonant second-harmonic and hyper-Raman scattering in a CdS quantum-dot system are reported. Two maxima have been found in the related two-photon excitation spectra near the fundamental absorption region. Relative to the one-photon absorption spectrum, the maxima are more pronounced and shifted in energy. The result has revealed quantum-confined electron-hole pair states with a total angular momentum of odd number. Effective masses in the quantum dots have been estimated.

Semiconductor nanocrystals, or the so-called quantum dots, with the radius R_0 comparable to or smaller than the exciton Bohr radius of the corresponding bulk crystal, are of great interest, because of unusual electronic structure and optical properties. In principle, due to the size-confinement effect in quantum dots, the energy spectra of quasiparticles, such as electrons, holes, phonons, and excitons, are transformed. Moreover, the confinement also modifies the interactions between the quasiparticles and external field, and between the quasiparticles themselves. In this connection, studies of such interactions, together with the inherent electronic structure, are of considerable importance. In addition, the systems containing quantum dots are expected to be promising materials for some applications in optoelectronics.

Up to now, a variety of experimental methods has been used for studies of semiconductor quantum dots: one-photon[1,2] and two-photon[3] absorption (OPA and TPA, respectively), resonant Raman scattering (RRS),[4,5] low-frequency Raman scattering,[5,6] photoluminescence,[7] four-wave mixing,[8] nonlinear bleaching,[9] and pump-and-probe technique.[10] Nonetheless, the nature of quantum dots is yet to be understood. This is partly due to the fact that the quality of the available samples is not high enough; among the related problems, for example, defects and surface interactions, a dot-size and dot-shape distribution is most crucial, since it causes large inhomogeneous broadening, as typically seen in the OPA spectra. That is why spectroscopic methods implying selection rules different from those of OPA are required. In particular, the methods of nonlinear optical spectroscopy, e.g., resonant hyper-Rayleigh scattering, or second-harmonic scattering (RSHS) (Ref. 11) and resonant hyper-Raman scattering (RHRS) by optic phonons,[12] are expected to be advantageous for clarifying not only the electronic structure, but the electron-phonon interaction as well. It should be noted that the selection rules in the RSHS and RHRS processes are different from those in RRS. The frequency w_s of the RHRS signal is given by the relation $w_s = 2w_0 - w_p$, where w_p and w_0 are the frequencies of phonon and incident photon, respectively. However, no attention has been given to RSHS and RHRS measurements in quantum-dot systems, except for the first observation of the effects in CdS_xSe_{1-x} quantum dots by two of the authors who used incident light with one wavelength.[13]

In this paper, the results of the observation of the RSHS and RHRS phenomena in a CdS quantum-dot system with the use of a wavelength-tunable laser are reported. In the experiment, the laser could be tuned so that the double frequency of excitation light fell in the region of the lowest-energy transitions generating electron-hole pairs. The CdS nanocrystals were grown in a multicomponent silicate glass by diffusion phase decomposition of a supersaturated solid solution of the basic constituents under secondary heat treatment. In this case, the size distribution of the crystallites can be described in terms of the Lifshitz-Slesov model.[14] The average dot radius R_0 of 2.0 nm and the OPA peak positions (Table I) were determined from the OPA spectrum, using a fitting procedure described in Ref. 2, with the Lifshitz-Slesov size distribution, the transition linewidth $\Gamma = 80$ meV, and the sole fitting parameter R_0. This R_0 value was supported by the result of a small-angle x-ray-scattering measurement (1.8 ± 0.1 nm). Consequently, the confinement effect should be important in the system under consideration because the exciton Bohr radius for CdS bulk crystal is 3.2 nm. A few rectangular plates, from 0.2 to 3.0 mm in thickness, cut from a large ingot were used as samples.

The RHRS and RSHS were excited by a pulsed Ti:sapphire laser. The incident photon energy was varied from 1.35 to 1.72 eV. The laser beam of 1 kW peak power, 30 ns pulse

TABLE I. The peak positions observed in the OPA, RSHS, and RHRS excitation spectra, and the relative shifts (eV).

OPA	RSHS	RHRS	Shifts
2.849	2.882	2.882	0.033 ± 0.005
3.22	3.18	3.16	0.04 ± 0.01 (0.06 ± 0.02)

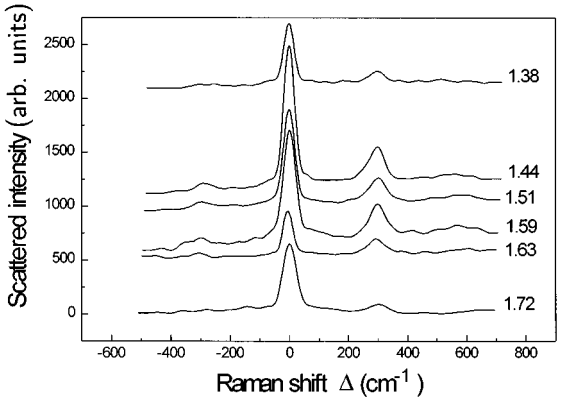

FIG. 1. Hyperscattering spectra in a CdS quantum-dot system for a number of incident photon energies (as denoted). The frequency origin corresponds to $\Delta = 2w_0 - w_s$. The band with the $\Delta = 0$ represents the RSHS and the band with the $\Delta = 305\ \mathrm{cm}^{-1}$ is the Stokes RHRS involving one LO phonon.

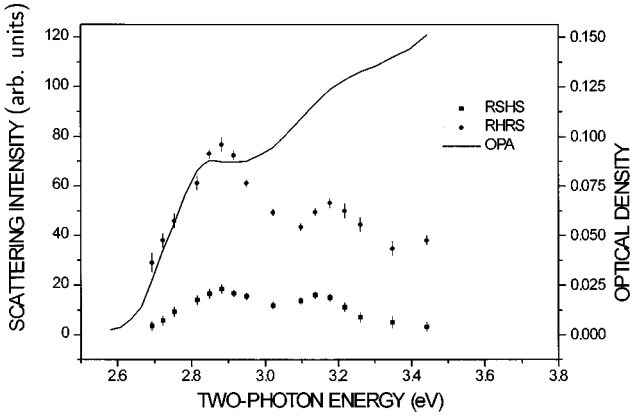

FIG. 2. Excitation spectra of the RHRS ($\Delta = 305\ \mathrm{cm}^{-1}$) and the RSHS ($\Delta = 0$) for a CdS quantum-dot system in the range of low-energy electron-hole transitions. Each point is averaged over three independent measurements. The OPA spectrum of the specimen 0.3 mm thick is also shown for comparison.

duration, and 3 kHz repetition rate was focused on a specimen $5 \times 8 \times 3\ \mathrm{mm}^3$ in size by using an achromatic lens with a focal length of 28 mm. The experiment was performed in the *x*(*yy, unspecified*)*z* incident-scattered light geometry (Porto's notation). The 90° scattered radiation was collected by a quartz lens, then dispersed with a single-grating monochromator (Ritsu Co., MC-25N) and detected with an optical multichannel detector (Tracor-Northern Co., TN 6133) cooled to $-30\,^{\circ}\mathrm{C}$. The spectral resolution of the measurements was about $25\ \mathrm{cm}^{-1}$. To avoid a possible contribution to the intrinsic RSHS signal from the second-harmonic light generated from the sample surfaces, a special mask was used. The correction for reabsorption was made in the ordinary way, taking into account the 0.1-mm path length of scattered light inside the specimen. All of the measurements were carried out at room temperature.

Figure 1 shows the typical scattering spectra observed for a number of incident photon energies. All of the spectra are plotted relative to $2w_0$. In each spectrum, the RSHS signal emerging from the CdS dots can be seen at the frequency $2w_0$, or with the zero Raman shift $\Delta = 0$ ($\Delta = 2w_0 - w_s$). Another spectral line with $\Delta = 305\ \mathrm{cm}^{-1}$ is also well pronounced. This line can be assigned to the RHRS signal from one LO phonon, clearly indicating that the electron-phonon coupling of the Fröhlich type is important in the process.

Figure 2 shows the RSHS and RHRS excitation spectra, i.e., the plots of the relative signal intensities as a function of $2w_0$, with the correction for reabsorption of scattered light and spectral response of the instrument. The OPA spectrum is also shown for comparison. It is evident from Fig. 2 that both RSHS and RHRS signals show resonant enhancement near the fundamental absorption (OPA) region. This confirms that the RSHS and RHRS signals originate from the CdS dots. Noticeably, each of the RSHS and RHRS excitation profiles exhibits two maxima, more pronounced than those in the OPA spectrum. Moreover, it is important to note that the second resonant maximum manifests itself in contrast to the RRS spectrum,[4,5] where only one resonance peak is observed around the lowest OPA peak. A detailed comparison reveals that the peak energies of the RSHS and RHRS excitation spectra, almost coincident with each other for the lower ones, deviate significantly from those of the OPA. Namely, the lower-energy maxima are shifted to the blue side, whereas the higher-energy maxima are shifted to the red side relative to the corresponding OPA peaks. The magnitudes of these shifts and the resulting peak energies are listed in Table I.

Now consider the results in more detail. First we show that each maximum is related to the two-photon resonant excitation of electron-hole pair states in the quantum-confined ''conduction'' and ''valence'' bands. These states are not revealed in the OPA. It is well known that size confinement induces splitting of each continuous conduction (valence) band to discrete levels.[15] If a simple two-band model with spherical potential is adopted for simplicity, then each discrete level corresponds to definite numbers of angular momentum l and submagnetic moment m. In the case of infinite potential barrier,[15] the wave function and energy of electronic state are expressed as

$$\Psi_{nlm}^{e(h)} = \mathscr{R}_{nl}(r) Y_{lm}(\varphi,\theta), \quad \mathscr{R}_{nl}(r) = \sqrt{\frac{2}{R_0^3}} \frac{j_l(\phi_{nl} r/R_0)}{j_{l+1}(\phi_{nl})},$$

$$E_{nl}^{e(h)} = \pm \left(\frac{E_g}{2} + \frac{\hbar^2 \phi_{nl}^2}{2R_0^2 m_{e(h)}} \right), \tag{1}$$

where $Y_{lm}(\varphi,\theta)$, $j_l(x)$ are spherical harmonics and spherical Bessel functions, ϕ_{nl} is the nth root of the equation, $j_l(\phi_{nl}) = 0$, m_e and m_h are the electron and hole effective masses, and E_g is the energy gap of the bulk crystal. Within the framework of the above model and the dipole approximation, the selection rules can be derived for one-photon interband (*a* or *f*) and intraband (ib) transitions. (The notations *a* and *f* are referred to allowed and weakly allowed, or ''forbidden'' interband transitions, respectively.) According to the $\mathbf{k}\cdot\mathbf{p}$ perturbation theory, the amplitudes V of one-photon matrix elements for typical semiconductors satisfy the conditions

$$V_a \gg V_{\mathrm{ib}} > V_f. \tag{2}$$

The selection rules are the following: $n' = n$, $l' = l$, $m' = m$ for *a* transitions; $l' - l = \pm 1$, $m' - m = 0, \pm 1$ for *f* and ib

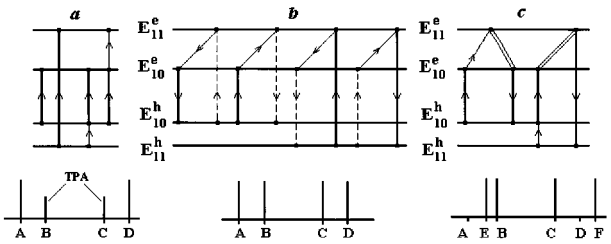

FIG. 3. Energy levels for a quantum dot and typical diagrams of the electronic transitions in the related OPA and TPA (a), RSHS (b), and RHRS (c) processes. Thick and thin solid lines correspond to a and ib transitions, respectively; dashed lines relate to f transitions, and double lines to phonon-induced transitions (see text). The sketch of the energy positions of expected resonances in the spectra are shown: $A=E^e_{10}-E^h_{10}$, $B=E^e_{10}-E^h_{11}$, $C=E^e_{11}-E^h_{10}$, $D=E^e_{11}-E^h_{11}$, $E=A+\hbar w_p$, $F=D+\hbar w_p$.

transitions, where n', l', m' (n, l, m) are the quantum numbers for the conduction (valence) band, or electron (hole) states. Obviously a transitions make the main contribution to the OPA, so that the lower- and higher-energy OPA peaks can be assigned to the a transitions from the valence-band state with $n=1$, $l=0$ to the conduction-band state with $n'=1$, $l'=0$ (energy position A) and from $n=1$, $l=1$ to $n'=1$, $l'=1$ (energy position D), respectively [Fig. 3(a)]. The TPA process involves both a and ib transitions, responsible for the two TPA peaks B and C, as shown in Fig. 3(a). At the same time, the RSHS is produced by three successive transitions, a combination of a, f, and ib transitions. The related typical diagrams of the transitions resulting in four energy resonances are shown in Fig. 3(b). Similarly, the typical diagrams showing four resonances for the RHRS are presented in Fig. 3(c). It should be noted that two of the four RHRS resonances coincide with two of the RSHS or two TPA resonances, but the other two are different, because unlike the RSHS, the RHRS involves electron-phonon interaction of Fröhlich type. Note that the off-diagonal matrix elements of the electron-phonon interaction make the major contribution to the RHRS, since the diagonal matrix elements between the electron states and those between the hole states cancel each other. Then, for the RHRS process, two a transitions and one ib transition should be taken into consideration, resulting in a relative increase in the RHRS amplitude as compared to the RSHS amplitude. As can be seen from Fig. 1, the intensities of the RHRS and RSHS signals are of the same order of magnitude, confirming the above statements. This situation is quite different from the well-known relationship between resonant Raman and Rayleigh scattering.

The reason why only two resonant peaks have been observed instead of the four peaks predicted theoretically may be as follows: due to the above-mentioned large inhomogeneous broadening, one wider peak, rather than two narrow peaks, occurs at the midpoint between the corresponding two closely positioned resonant energies. Since m_h is much larger than m_e, four resonant energies can be classified into two groups separated from each other. The middle energy of the lower-energy group, or of the pair states with $n=1$, $l=0$ and $n'=1$, $l'=0$ (the lowest peak, A) and $n=1$, $l=1$ and $n'=1$, $l'=0$ (B), is shifted to the higher-energy side regarding peak A, while the middle energy of the higher-energy group (C and D) is shifted to the higher-energy side regarding C. As for these shifts, this is indeed the case observed experimentally. However, on the quantitative level, the relative shifts between the RSHS and RHRS peaks are not necessarily distinguished. For the first peak, no appreciable difference can be recognized, and for the second peak, the maximum energy is lower in the RHRS than in the RSHS and, besides, the observed shift is larger than that of the first group, 33 meV. This may be due to a large uncertainty in estimating the second OPA peak position. In this connection, it should be also pointed out that the situation with the second resonance position is more complicated if the other pair states, such as those with $n'=1$, $l'=2$, are taken into account. Below, attention will be focused on the first resonant peak, particularly the RSHS peak, which is more reliable from the experimental standpoint. This is partly because the RSHS process is simpler than RHRS in nature and the excitation spectrum is more pronounced for RSHS than for RHRS. From Eq. (1) with $R_0=2.0$ nm, the effective masses of electron and holes can be evaluated as $m_h/m_0=1.4$ and $m_e/m_0=0.3$, respectively. No information on these quantities for CdS quantum dots is available; the bulk (wurtzite) values are reported as $m_{h\parallel}/m_0=5$, $m_{h\perp}/m_0=0.7$, and $m_e/m_0=0.2$.

Now the results are discussed in comparison with data obtained previously. First, the present excitation spectra differ from the TPA spectrum[3] observed at 10 K for a similar CdS quantum-dot system. In that work, two TPA peaks were detected as well, but their energies coincided with those of the OPA spectrum; this coincidence was interpreted as being caused by valence-band mixing and thereby intrinsic. The reason for the discrepancy between the TPA results and our data is not yet completely clear. It should be noted that the RSHS and RHRS excitation peaks, although observed at 300 K, are more pronounced than the TPA peaks. It is the fact that the resonant scattering phenomena under consideration provide a kind of modulation spectroscopy that makes only the relevant electronic states prominent, as compared to the TPA. This is usually the case for the RRS as compared to the OPA. At low temperatures, the exciton effects become relatively more important, but this aspect is a less probable cause of the discrepancy in question. Next, the selection rules for the RRS and RHRS are quite different, thereby providing the complementary spectroscopic methods. In the case of quantum-dot systems, the RHRS can give more information than the RRS, as already described for CdS dots.[4,5] A comparison of both results should allow one to gain an insight into the mechanism of electron-phonon interaction in quantum-dot systems. The related consideration, however, will be presented in a separate paper.

Finally, the estimations of effective masses may be very crude, as obtained in the framework of the rather simplified two-band model with an infinite spherical potential. To analyze the RSHS and RHRS excitation spectra quantitatively, a theory of the hyperscattering phenomena in a quantum-dot system is needed. The theory should be based on a sophisticated model taking into account a more realistic valence-band structure,[16] the confinement-induced valence-band mixing effect,[17] and a finite potential as well. Such a theoretical work is now in progress. In conclusion, we have shown that

both the RSHS and RHRS signals can be easily observed in the fundamental absorption range for a typical CdS quantum-dot system, and that the off-diagonal Fröhlich interaction predominantly governs the RHRS process. From the RSHS and RHRS excitation spectra, we have clarified two electron-hole pair states with the total angular momentum, equal to unity, unobservable in the OPA. Thus we have demonstrated that the resonant hyperscattering phenomena provide a useful spectroscopic tool for studying quantum-dot systems. The techniques are complementary to the TPA spectroscopy, but may be simpler and more direct than the emission-probed TPA.

This work was partly supported by the ISF through Grants Nos. NGL000 and NGL300.

[1] A. I. Ekimov and A. A. Onushchenco, Pis'ma Zh. Éksp. Teor. Fiz. **40**, 337 (1984) [JETP Lett. **40**, 1136 (1984)].

[2] Ph. Roussignol, D. Ricard, and Chr. Flitzanis, Appl. Phys. B **51**, 437 (1990).

[3] K. I. Kang, B. P. McGinnes, Sandalphon, Y. Z. Hu, S. W. Koch, N. Peyghambarian, A. Mysyrowicz, L. C. Liu, and S. H. Risbod, Phys. Rev. B **45**, 3464 (1992).

[4] A. V. Baranov, Ya. S. Bobovich, and V. I. Petrov, Opt. Spektrosk. **65**, 1066 (1988) [Opt. Spectrosc. **65**, 628 (1988)]; A. P. Alivisatos, T. D. Harris, P. J. Carroll, M. L. Steigerwald, and L. E. Brus, J. Chem. Phys. **90**, 3463 (1989); M. C. Klein, F. Hache, D. Ricard, and C. Flitzanis, Phys. Rev. B **42**, 11 123 (1990); A. V. Baranov, Ya. S. Bobovich, and V. I. Petrov, Solid State Commun. **83**, 957 (1992).

[5] A. V. Baranov, Ya. S. Bobovich, and V. I. Petrov, J. Raman Spectrosc. **24**, 767 (1993).

[6] B. Champagnon, B. Andianosolo, and E. Duval, J. Chem. Phys. **74**, 5237 (1991).

[7] M. G. Bawendi, W. L. Wilson, L. Rothberg, P. J. Caroll, T. M. Jedju, M. L. Steigerwald, and L. E. Brus, Phys. Rev. Lett. **65**, 1623 (1990).

[8] D. W. Hall and N. F. Borrelli, J. Opt. Soc. Am. B **5**, 1650 (1988).

[9] Y. Wang, N. Herron, W. Mahler, and A. Suna, J. Opt. Soc. Am. B **6**, 808 (1989).

[10] Y. Z. Hu, S. W. Koch, M. Lindberg, N. Peyghambarian, E. L. Pollock, and F. F. Abraham, Phys. Rev. Lett. **64**, 1805 (1990).

[11] F. Minami, K. Inoue, Y. Kato, K. Yoshida, and K. Era, Phys. Rev. Lett. **64**, 3708 (1991).

[12] K. Inoue, K. Yoshida, F. Minami, and Y. Kato, Phys. Rev. B **45**, 8807 (1992).

[13] A. V. Baranov, Ya. S. Bobovich, N. I. Grebenshcikova, V. I. Petrov, and M. Ya. Thenter, Opt. Spektrosk. **60**, 1108 (1986) [Opt. Spectrosc. **60**, 685 (1986)].

[14] I. M. Lifshitz and V. V. Slesov, Zh. Éksp. Teor. Fiz. **35**, 497 (1958) [Sov. Phys. JETP **35**, 331 (1959)].

[15] Al. L. Efros and A. L. Efros, Fiz. Tekh. Poluprovodn. **16**, 1209 (1982) [Sov. Phys. Semicond. **16**, 772 (1982)].

[16] G. B. Grigoryan, E. M. Kazaryan, Al. L. Efros, and T. V. Yazeva, Fiz. Tverd. Tela (Leningrad) **32**, 1772 (1990) [Sov. Phys. Solid State **32**, 1772 (1990)].

[17] J. B. Xia, Phys. Rev. B **40**, 8500 (1989); K. J. Vahala and P. C. Sercel, Phys. Rev. Lett. **65**, 239 (1990).